A Dispatching Method for Integrated Energy System Based on Dynamic Time-interval of Model Predictive Control

Xun Dou, *Member*, *IEEE*, Jun Wang, *Member*, *IEEE*, Zhen Wang, Lijuan Li, Linquan Bai, Shuhui Ren, and Min Gao

***Abstract*—In integrated energy systems (IESs), traditional fixed time-interval dispatching scheme is unable to adapt to the need of dynamic properties of the transient network, demand response characteristics, dispatching time scales in energy sub-systems and renewable power uncertainties. This scheme may easily result in uneconomic source-grid-load-storage operations in IES. In this paper, we propose a dispatching method for IES based on dynamic time-interval of model predictive control (MPC). We firstly build models for energy sub-systems and multi-energy loads in the power-gas-heat IES. Then, we develop an innovative optimization method leveraging trajectory deviation control, energy control, and cost control frameworks in MPC to handle the requirements and constraints over the time-interval of dispatching. Finally, a dynamic programming algorithm is introduced to efficiently solve the proposed method. Experiments and simulation results prove the effectiveness of the method.**

***Index Terms*—Dispatching scheme, dynamic time-interval, integrated energy system, model predictive control.**

NOMENCLATURE

β_{com}	The coefficient of compressor
η_{CHP}	The efficiency of combined heat and power (CHP)
η_{HE}	The efficiency of heat exchanger (HE)
η_T	The efficiency of power transformer (T)
η_{HR}	The efficiency of heat recovery (HR)
η_{AC}	The efficiency of absorption refrigeration (AC)
η_{P2G}	The efficiency of P2G
η_{EC}	The efficiency of electric refrigeration (EC)
ξ_t	The decision index of dynamic time-interval
ς_t	The correction index of reference trajectory
ϕ_{CHP}	The thermoelectric of CHP
$\lambda_{e,1}$, $\lambda_{e,2}$, $\lambda_{e,3}$	The input power distribution ratios
$\lambda_{g,1}$, $\lambda_{g,2}$	The input natural gas distribution ratios
Ω_m	Index of the node connected to node m
$\omega_{c,t}^f$	The real time intraday reference track
$\omega_{c,t}^r$	The real time actual track
ρ	The hot water density
ρ_u^e	The incremental adjustment cost of the u^{th} generator
ρ_v^g	The incremental adjustment cost of the v^{th} gas source
θ_{mn}	The voltage phase angle difference between nodes m and n
$\Delta p(k)$	The control incremental
$\Delta \boldsymbol{p}(k)$	The control increment matrix
$\boldsymbol{A}$	A unit matrix of 1 row and T column
C	The specific heat capacity of hot water
$\boldsymbol{C}$	The cost coefficient matrix
c_l	The l^{th} resource cost control factor
C_{mn}	The constant related to the efficiency, temperature, length, inner diameter, and compression factor of the pipe mn
$C(k)$	The cost of supplying equipment to the load
$\boldsymbol{C}(k)$	The cost matrix for supplying equipment to the load
C_u^e	The power generation cost of the u^{th} generator

Manuscript received: December 27, 2019; accepted: July 17, 2020. Date of CrossCheck: July 17, 2020. Date of online publication: September 18, 2020.

This work was supported in part by National Key R&D Program of China (No. 2018YFB0905000), National Natural Science Foundation of China (No. 61873121) and Science and Technology Project of State Grid Corporation of China (No. SGTJDK00DWJS1800232).

X. Dou, J. Wang, Z. Wang, L. Li, and S. Ren are with the College of Electrical Engineering and Control Science, Nanjing Tech University, Nanjing, China (e-mail: dxnjut@njtech.edu.cn; wjnjut@163.com; 2629675471@qq.com; ljli@njtech.edu.cn; 360167160@qq.com).

L. Bai (corresponding author) is with the Department of Systems Engineering and Engineering Management, University of North Carolina at Charlotte, Charlotte, USA (e-mail: linquanbai@uncc.edu).

M. Gao is with Falcon Computing Solutions, 10880 Wilshire Blvd Suite 1132, Los Angeles, CA 90024, USA (e-mail: mingao@falcon-computing.com).

DOI: 10.35833/MPCE.2019.000234

C_v^g	The natural gas price of the v^{th} gas source
C_s^d	The load control cost of the s^{th} energy
$E_{u,t}$	The active output of the u^{th} generator at time t
$E_{u,t}^r$	The actual output of the u^{th} generator at time t
$E_u^{\max}$, $E_u^{\min}$	The upper and lower limits of the active power output of the u^{th} generator
f	The water flow in heating pipes
$F_{m,t}^{GS,in}$, $F_{m,t}^{GS,out}$	The gas flows extracted and injected by gas energy storage at node m at time t
$G_{v,t}^r$	The actual gas production of the v^{th} gas source at time t
G_{mn}, B_{mn}	The conductance and susceptance between nodes m, n
$G_{v,t}$	The gas production rate of the v^{th} gas source at time t
$h_{m,t}^L$	The consumption of heat in node m at time t
i	The index of the predicted time domain
j	The index of the control time domain
k	The control time step
$L_{mn,t}$, L_t	The pipe storage in pipe mn and all pipe at time t
L_e	The load consumption of electricity
L_g	The load consumption of gas
L_h	The load consumption of heat
L_c	The load consumption of cooling
l	The index of demand side and system side resource
m, n, o	The indexes of the bus of one line in system
M	The number of the control time domain
M_{mn}	The constant related to the length, radius, temperature, gas density, compression factor of the pipe mn
N	The number of the predicted time domain
$\boldsymbol{P}$	The decision time period and the predicted time domain control amount matrix at time t
$p_{lT,t}$	The amount of regulation of the l^{th} demand side and system side resource in the predicted time domain T at time t
$P_{m,t}^{EL}$	The load active power of node m at time t
$P_{s,t}^{LS}(k)$	The actual value of the minute load of the s^{th} energy load at time t
P_E	The consumption of electricity
P_G	The consumption of gas
$P_{mn,t}$	The active power of the line between nodes m and n at time t
$P_{m,t}^w$, $P_{m,t}^{CHP}$, $P_{m,t}^{ES,in}$, $P_{m,t}^{ES,out}$, $P_{m,t}^{P2G}$	The active power of wind turbine, CHP, energy storage discharge, energy storage charging and P2G consumption of node m at time t
$p_m^{\max}$, $p_n^{\min}$	The upper and the lower limits of pressure at node m and n
$p_{m,t}$, $p_{n,t}$	The pressure values of the first and last nodes m and n at time t
$P_{mn}^{\max}$, $P_{mn}^{\min}$	The active power transmission upper and lower limits of the line between nodes m and n at time t
$\tilde{P}_{mn,t}$	The average pressure of the pipe mn at time t
$P_{s,t}^L(k)$	The predictive value of the minute load of the s^{th} energy load at time t
$\boldsymbol{Q}$, $\boldsymbol{R}$, $\boldsymbol{S}$	The weight matrices in different scenarios
$Q_{m,t}^{P2G}$, $Q_{m,t}^{CHP}$	The supply flow rate of P2G and CHP at node m at time t
$Q_{n,t}^g$, $Q_{o,t}^g$	The mass flows in and out the pipe m at time t
$Q_{m,\max}^N$, $Q_{m,\min}^N$	The upper and lower limits of the natural gas supply flow rate of the gas well at node m
$Q_{m,t}^{GL}$	The gas load on node m at time t
$Q_u^{\max}$, $Q_u^{\min}$	The upper and lower limits of the reactive power output of the u^{th} generator
$Q_{m,t}^{EL}$	The load reactive power of node m at time t
$Q_{mn,t}$	The reactive power of the line between nodes m and n at time t
$Q_{u,t}$	The rective power of the u^{th} generator at time t
$\tilde{Q}_{mn,t}$	The average flow rate flowing through the pipe mn at time t
$Q_{mn,t}^{in}$, $Q_{mn,t}^{out}$	The flow rate into and out of the natural gas pipeline mn at time t
$Q_{m,t}^N$	The gas supply flow rate at the node m at time t
R	The thermal resistance per unit length of heating pipe
RU_u, RD_u	The maximum active power rise and decrease of the u^{th} generator
s	The index of the energy type
$S_{r,t}$	The global cost of the decision period and the predicted time domain at time t
$S_{w,t}$	The global cost of reference trajectory
S_m^{pipe+}, S_m^{pipe-}	The indexes of pipes connected to node m and starting and ending from node m
t, T	The indexes of the time interval
$T_{n,t}^O$	The hot water outlet temperature in the pipe n in time t
$T_{o,t}^I$	The hot water inlet temperature in the pipe o in time t

T_s, T_e, T_a	The head temperature, x temperature and outside temperature of the heating pipe
$T^g_{m,t}$, $T^h_{m,t}$	The supply and return temperatures of water in node m at time t
$T^g_{\max}$, $T^h_{\max}$	The upper limits of water supply and return temperature
$T^g_{\min}$, $T^h_{\min}$	The lower limits of water supply and return temperature
u	The index of the generator
U	The number of the generator
$\hat{u}_P(k+i)$	The output prediction link including the active output and gas production of the equipment
$\hat{\boldsymbol{U}}_P(k+1)$	The predictive output matrix
v	The index of the natural gas source
V	The number of the natural gas source
$V_m^{\max}$, $V_m^{\min}$	The upper and lower limits of the allowable voltage value of the node m
$V_{m,t}$	The node voltage of node m at time t
$w(k+i)$	The reference track for real-time dispatching including the active output and gas production of the equipment
$\boldsymbol{W}(k+1)$	The reference track matrix
x	The distance from the top end of the heating pipe
Z	The day-ahead economic dispatching cost

I. Introduction

With the massive integration of renewable energy, integrated energy systems (IESs) become important to achieve efficient use of energy [1]. The optimal dispatching of IESs is the key technology to achieve coordinated and complementary utilization of various types of energy such as power, heat, and natural gas [2]. In the optimal dispatching, the efficiency of the dispatching scheme largely depends on the accuracy of load and renewable forecasting within the dispatching period. Usually, the forecasting accuracy decreases with the increase of dispatching time scale. The impact of the forecasting errors on the optimal dispatching can be mitigated by decomposing the dispatching period into multiple time scales [3]. Therefore, it is necessary to study the multi-section coordinated optimal dispatching of IES with multiple time scales. However, electric power distribution system, natural gas networks, and thermal networks have different response rates to the dispatching signals [4]. The power system has the smallest inertia and fastest response rate. The response rate of natural gas distribution system is slower due to the gas transportation speed and pipeline linepack. The response rate of district heating/cooling system is the slowest. Therefore, the sub-systems in IES have significant difference in dynamic response characteristics. In addition, the dispatchable resources in different sub-systems are different in the same time section. These factors pose challenges to the selection of the dispatching cycle of IES. If the dispatching period is too long, there could be a significant error between the dispatching plan and the real system operation conditions. If the dispatching period is too short, it will add the computation and control burden onto system operation. Therefore, for IES dispatching with multiple time scale, it is urgent to choose reasonable dispatching time and realize the efficient use of energy resources in IES through necessary and accurate time section dispatching. However, most of these optimal dispatching methods control a certain time section or multiple time scales, which still belongs to static optimization [3]. For the fast and slow dynamic characteristics of electric power distribution system, natural gas distribution systems and district heating system with different time scales, there are also related studies that can perform intra-day/ultra-short-term rolling optimization dispatching on specific systems such as electricity-gas [3], electricity-heat [4]. However, it is still an open-loop optimal dispatching method. The accuracy of load prediction can be improved by dividing the time scale, but the impacts of actual system operation on the optimal control process [3] are rarely considered.

Existing works on IES optimal dispatching are developed based on the physical models of individual and coupled unit equipment [5], economic model [6] and steady-state flow model of power, natural gas, and thermal sub-systems [7]. To achieve optimal dispatching of integrated energy for IESs such as electricity-gas, electricity-heat [8], [9], an optimal dispatching strategy considering energy conversion equipment is proposed in [10] and [11]. To address the uncertainties of renewable energy such as wind power, robust optimization is applied in the optimal dispatching [12]. The day-ahead or intraday optimal dispatching plan is presented in [13] through mining the responses of the users to the information price. The partial load performance of CCHPs and the performance of ice-storage air-conditioners are modeled, and the cooling and electricity coordinated microgrid day-ahead scheduling and real-time dispatching models are established in [14]. In real-time scheduling, different time scale scheduling schemes are used for the scheduling of cooling and power to smooth out the fluctuation of renewable energy. Reference [15] presents the coordination of energy management of multi-energy systems composed of multiple energy agencies. The paper also proposes a distributed algorithm based on event triggering. The goal of energy agencies is achieved, collaborating to maximize daily social welfare and eliminate real-time load changes and fluctuations in renewable resources. Reference [16] proposes a new Energy Internet of energy management framework with multiple energy subjects. In order to solve the problems of power-heat-gas coupling, global constraint limits and nonlinear objective function faced by the optimal energy management of the Energy Internet, a novel distributed-consensus alternating direction method of multiplier algorithm is proposed. However, most of these methods are for a certain time or multi-time periods, which is static optimization [3]. To address dynamic characteristics of power systems, natural gas distribution systems, and district heating system at different time scales, intraday and ultra-short-term rolling optimizations are carried out based on economic dispatching for IESs [3], [17].

In view of the lack of robustness in open-loop optimal dis-

patching, the model predictive control (MPC) method is applied to optimal dispatching as a control method for system optimization. Different from the open-loop multi-time optimal dispatching method, MPC introduces the feedback and correction of state variables, which can correct the optimal dispatching deviation caused by forecasting errors. MPC can also obtain the optimal control signals of current and future time periods to minimize the differences between the future output and reference trajectory [18], [19], which is robust and immune to disturbances and errors.

MPC has been applied to frequency control in various grids such as home local area network (LAN) [20], microgrids [21], distribution networks [22], cogeneration microgrids [23], combined heat and power (CHP) systems [24]. It controls [25] and optimizes the dispatching in the field of power systems and IESs [26], which demonstrates good performance in stability control and system robustness [27]. However, a fixed time-interval base on a sequential rolling is used, and the trajectory deviation is applied as the performance index.

Considering that the fixed time-interval of dispatching is difficult to provide timely and accurately control when large errors occur in the system, we propose to establish the decision index of dynamic time-interval to solve the problem based on real system status. To address the uncertainties and forecasting errors in different time sections, we propose an MPC-based economic dispatching method for IESs at dynamic and hybrid optimization time scales to ensure global optimum based on the correction index of reference trajectory. The contributions of this paper are summarized as follows.

1) A decision index of dynamic time-interval is proposed to address large-scale forecasting errors and provide indicators for system operators whether the system needs to issue dispatching instructions.

2) A correction index of reference trajectory is proposed to address the deviations between the forecasting and actual system conditions to achieve the global optimal dispatching in the predicted time domain.

3) A dispatching method for IESs is proposed based on dynamic time-interval of MPC with trajectory deviation, control energy, and control cost as performance index, which will ensure sufficient adjustment margin for the performance index to meet the operation requirement in different scenarios.

The structure of this paper is as follows. Section II establishes a dispatching method for IES based on dynamic time-interval of MPC. Section III builds an IES model, including electric power distribution system, natural gas distribution systems and district heating system. In Section IV, the effectiveness of the proposed method is demonstrated by numerical examples. The effects of different performance index and different decision indexes of dynamic time-interval on the dispatching results are compared and analyzed. Section V summarizes the main findings of this paper.

II. Dispatching Model of IES Based on Dynamic Time-interval of MPC

A. Dispatching Principle

Based on day-ahead dispatching, we propose a real-time rolling optimization dispatching method based on dynamic time-interval of MPC. The principle is shown in Fig. 1. The day-ahead dispatching aims to minimize the operation cost and develop the hourly operation plan on the next day. The rolling optimization dispatching is based on the previous dispatching plan as the reference track $w(k+i)$, and the system actual operation output is used as the initial value for rolling optimization. According to the system state at time k, the system state is predicted based on the prediction model at time $k+1$, and the system state and output at time k constitute the output prediction block $\hat{u}_P(k+i)$. The output prediction block depends on the decision index of dynamic time-interval ξ_t. It is necessary to issue an instruction to modify the dispatching plan. Through the correction index of reference trajectory ς_t, it is determined whether the reference trajectory needs to be corrected.

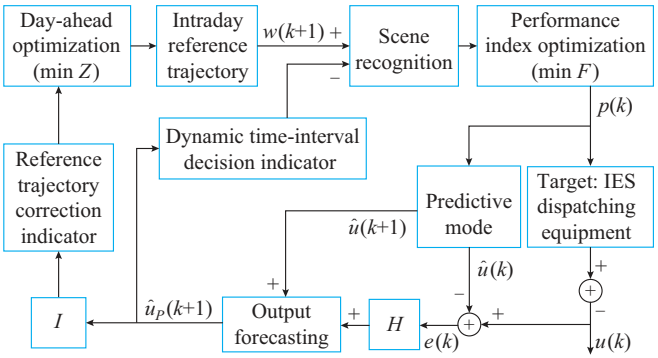

Fig. 1. Principle of IES dispatching method based on dynamic time-interval of MPC.

B. Day-ahead Dispatching Method

For the day-ahead economic dispatching method, the objective function is as follows:

$$\min Z = \sum_{t=1}^{T}\left(\sum_{u\in U} C_u^e E_{u,t} + \sum_{v\in V} C_v^g G_{v,t}\right) \tag{1}$$

C. Dispatching Model of IES

MPC is mainly composed of three parts: model prediction, rolling optimization, and feedback correction. Taking the system state at the start of dispatching as the initial state, based on the prediction model, we can obtain the optimal control plan by solving the optimal control problem for the future finite time duration [22], [28].

In this paper, the rolling forecasting values of active output and gas production are taken as the input variables. Actual measured values of the power generators and gas sources at the initial time are the initial value. Active power output and gas production adjustment in the time domain are used as the control variables to perform the rolling optimization. The improvement of dynamic time-interval mainly includes the improvement of performance index, decision index of dynamic time-interval, and correction index of reference trajectory.

1) Performance Index

The reference trajectory $w(k+i)$ and output prediction $\hat{u}_P(k+i)$ obtained by the day-ahead dispatching method are optimized according to the performance index after scenario

recognition. Performance metrics are the objective function of rolling optimization. The performance index function considers the trajectory deviation, control energy, and control cost, as shown in (2), and the matrix form is presented in (3).

$$\min F(k)=\sum_{i=1}^{N}\left(q_i\hat{u}_P(k+i)-w(k+i)\right)^2+\sum_{j=1}^{M}r_j\Delta p^2(k+j-1)+\sum_{j=1}^{M}s_jC^2(k+j-1) \tag{2}$$

$$\begin{cases}F=\left(\hat{\boldsymbol{U}}_p(k+1)-\boldsymbol{W}(k+1)\right)^{\mathrm{T}}\boldsymbol{Q}\left(\hat{\boldsymbol{U}}_p(k+1)-\boldsymbol{W}(k+1)\right)+\\ \quad\Delta\boldsymbol{P}^{\mathrm{T}}(k)\,\boldsymbol{R}\Delta\boldsymbol{P}(k)+\boldsymbol{C}^{\mathrm{T}}(k)\,\boldsymbol{S}\boldsymbol{C}(k)\\ \boldsymbol{Q}=\mathrm{diag}\{q_1,q_2,\ldots,q_N\}\\ \boldsymbol{R}=\mathrm{diag}\{r_1,r_2,\ldots,r_M\}\\ \boldsymbol{S}=\mathrm{diag}\{s_1,s_2,\ldots,s_M\}\end{cases} \tag{3}$$

The measured output and the reference trajectory include the active output and gas production of the device, and the difference between the real-time dispatching of the system and the current plan, which can be further expressed as:

$$\hat{u}_P(k+i)-w(k+i)=\sum_{u\in U}|E^r_{u,t}(k+i)-E_{u,t}(k+i)|+\sum_{v\in V}|G^r_{v,t}(k+i)-G_{v,t}(k+i)| \tag{4}$$

It is the deviation of the real-time dispatching of the total active output, gas production and future plans, which can be called as real-time deviation before the day.

As the incremental costs of the generator set and natural gas source are based on the planned day, the control incremental is expressed as:

$$\Delta p(k)=\sum_{u\in U}\rho^e_u\Delta p_{u,t}(k)+\sum_{v\in V}\rho^g_v\Delta p_{v,t}(k) \tag{5}$$

In (6), $C(k)$ includes generation supply costs and demand response costs through load control, which is the real-time dispatching cost.

$$C(k)=\sum_{u\in U}C^e_u(E_{u,t}(k)+\Delta p_{u,t}(k))+\sum_{v\in V}C^g_v(G_{v,t}(k)+\Delta p_{v,t}(k))+\sum_{s\in S}C^d_s|P^L_{s,t}(k)-P^{LS}_{s,t}(k)| \tag{6}$$

The acquisition of the schedule tracking is performed to detect changes in the minute-level load and the predicted load. The load control quantity of the demand response is obtained according to the load change of the detection time scale and the load change of the dispatching time scale.

2) Decision Index of Dynamic Time-interval

Further, we establish ξ based on the deviation rate of the total operation cost of IES in the time domain and the total operation cost under ξ_t during the period to be determined. The global cost is given by:

$$S_{r,t}=\boldsymbol{APC}=\begin{bmatrix}1 & 1 & \ldots & 1\end{bmatrix}\begin{bmatrix}p_{11,t} & p_{21,t} & \cdots & p_{I1,t}\\ p_{12,t} & p_{22,t} & \cdots & p_{I2,t}\\ \vdots & \vdots & & \vdots\\ p_{1T,t} & p_{2T,t} & \cdots & p_{IT,t}\end{bmatrix}\begin{bmatrix}c_1\\ c_2\\ \vdots\\ c_I\end{bmatrix} \tag{7}$$

ξ_t can be expressed as:

$$\xi_t=-\frac{S_{w,t}-S_{r,t}}{S_{w,t}} \tag{8}$$

When the dispatching optimized trajectory of MPC and reference trajectory deviation impact heavily on the global operation cost, the decision of dynamic time-interval will be triggered; the control interval will be changed; the time-interval of control will be optimized; and the dispatching instruction will be executed in advance. When the impact is small, the MPC-based optimization will not be triggered and unnecessary execution of instructions is reduced.

3) Correction Index of Reference Trajectory

When the actual operation condition is deviated from the predicted scenario, the reference trajectory based on day-ahead plan is not suitable to serve as an index. Therefore, we establish a correction index reference trajectory by comparing $\omega^r_{c,t}$ with the reference trajectory. The day-ahead dispatching plan mainly determines the optimal on/off status of the generators through unit commitment. Therefore, if a large deviation occurs at the current time, the unit commitment should be adjusted. ς_t can be expressed as:

$$\varsigma_t=\frac{|\omega^r_{c,t}-\omega^f_{c,t}|}{\omega^f_{c,t}}=\frac{\sum_{u\in U}|E^r_{u,t}-E_{u,t}|}{\sum_{u\in U}E_{u,t}}+\frac{\sum_{v\in V}|G^r_{v,t}-G_{v,t}|}{\sum_{v\in V}G_{v,t}} \tag{9}$$

D. Dispatching Process for IES Based on Dynamic Time-interval of MPC

Dispatching process for IES based on dynamic time-interval of MPC is depicted in Fig. 2.

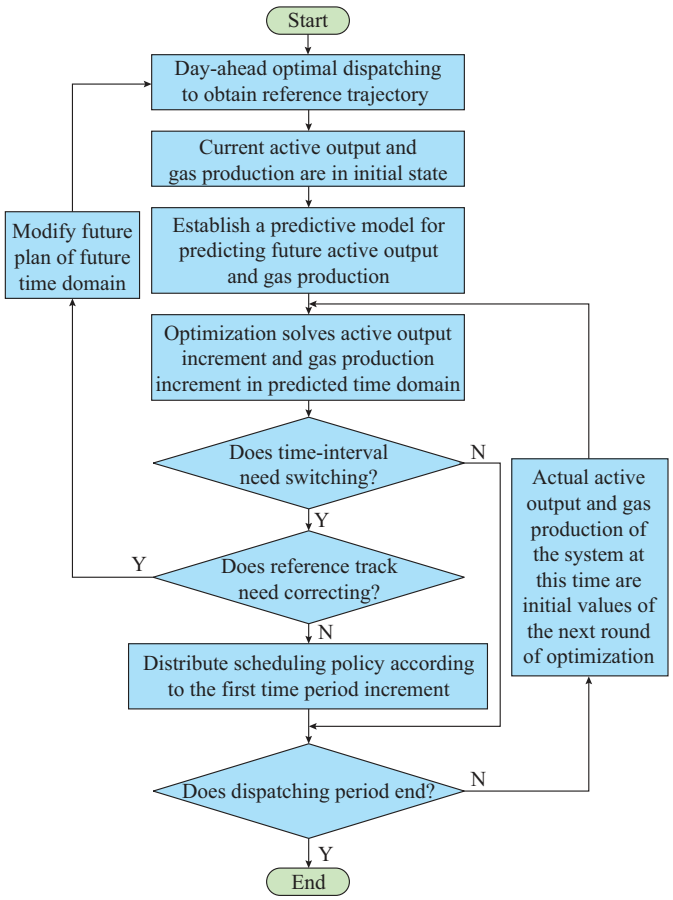

Fig. 2. Flow chart of IES dispatching based on dynamic time-interval of MPC.

In the real-time rolling optimization, the control schedules are obtained by solving the optimal dispatching problem in the future time domain based on the initial state of the current system conditions and MPC method [28]. Then, we will determine if it is necessary to change the time-interval of dispatching based on the current state and the decision index of dynamic time-interval. The correction index of reference trajectory determines whether the reference trajectory needs to be corrected and performs a rolling optimization

III. Constraints of Power-Gas-Heat IES

A. Unit Constraint of Energy Conversion

The energy conversion devices in IES link the power system, natural gas distribution system, and district heating system together. In this paper, the energy conversion devices include CHP, power transformer (T), heat exchanger (HE), heat recovery (HR), power to gas (P2G), electric refrigeration (EC) and absorption refrigeration (AC). The energy balance equation of the energy conversion unit is expressed as:

$$\begin{bmatrix} L_e \\ L_g \\ L_h \\ L_c \end{bmatrix} = \begin{bmatrix} \lambda_{e,1} & \lambda_{g,1}\eta_T\eta_{CHP} \\ \lambda_{e,2}\eta_{P2G} & \lambda_{g,2} \\ 0 & \lambda_{g,1}\eta_{HE}\phi_{CHP}\eta_{\mathrm{CHP}} \\ \lambda_{e,3}\eta_{EC} & \lambda_{g,1}\eta_{AC}\eta_{HR}\eta_{HE}\phi_{CHP}\eta_{CHP} \end{bmatrix} \begin{bmatrix} P_e \\ P_g \end{bmatrix} \tag{10}$$

B. Constraints of Electric Power Distribution System

The power system model mainly includes three-phase power flow constraints, power balance constraints, generator set output constraints, node voltage constraints, line power constraints, and generator set climbing constraints. The details of the model can be found in [29], [30].

$$\sum_{n\in\Omega_m} P_{mn,t} = \sum_{u\in\Omega_m} E_{u,t} + P^{w}_{m,t} + P^{CHP}_{m,t} + P^{ES,in}_{m,t} - P^{ES,out}_{m,t} - P^{P2G}_{m,t} - P^{EL}_{m,t} \tag{11}$$

$$\sum_{n\in\Omega_m} Q_{mn,t} = \sum_{u\in\Omega_m} Q_{u,t} - Q^{EL}_{m,t} \tag{12}$$

$$V^{\min}_m \le V_{m,t} \le V^{\max}_m \tag{13}$$

$$\sum_{n\in\Omega_m} P_{mn,t} - V_{m,t}\sum_{n\in\Omega_m} V_{n,t}\left(G_{mn}\cos\theta_{mn} + B_{mn}\sin\theta_{mn}\right) = 0 \tag{14}$$

$$\sum_{n\in\Omega_m} Q_{mn,t} - V_{m,t}\sum_{n\in\Omega_m} V_{n,t}\left(G_{mn}\sin\theta_{mn} - B_{mn}\cos\theta_{mn}\right) = 0 \tag{15}$$

$$-P^{\max}_{mn} \le P_{mn,t} \le P^{\max}_{mn} \tag{16}$$

$$E^{\min}_u \le E_{u,t} \le E^{\max}_u \tag{17}$$

$$Q^{\min}_u \le Q_{u,t} \le Q^{\max}_u \tag{18}$$

$$E_{u,t} - E_{u,t-1} \le RU_u \tag{19}$$

$$E_{u,t-1} - E_{u,t} \le RD_u \tag{20}$$

C. Constraints of Natural Gas Distribution System

Modelling of natural gas distribution system need to consider Weymouth equations, including pipeline flow constraints, gas source point constraints, flow balance constraints, compressor constraints, pipe storage constraints, and node pressure constraints. The details of the model can be found in [30].

$$\tilde{Q}_{mn,t}\left|\tilde{Q}_{mn,t}\right| = C^2_{mn}\left(p^2_{m,t} - p^2_{n,t}\right) \tag{21}$$

$$\tilde{Q}_{mn,t} = \frac{1}{2}\left(Q^{in}_{mn,t} + Q^{out}_{mn,t}\right) \tag{22}$$

$$Q^{N}_{m,\min} \le Q^{N}_{m,t} \le Q^{N}_{m,\max} \tag{23}$$

$$0 = Q^{N}_{m,t} + \sum_{n\in\Omega_m} Q_{mn,t} + Q^{P2G}_{m,t} + F^{GS,out}_{m,t} - F^{GS,in}_{m,t} - Q^{GL}_{m,t} - Q^{CHP}_{m,t} \tag{24}$$

$$p_{n,t} \le \beta_{com}\, p_{m,t} \tag{25}$$

$$L_{mn,t} = M_{mn}\tilde{P}_{mn,t} \tag{26}$$

$$\tilde{P}_{mn,t} = \frac{1}{2}\left(p_{m,t} + p_{n,t}\right) \tag{27}$$

$$L_{mn,t} = L_{mn,t-1} + Q^{in}_{mn,t} - Q^{out}_{mn,t} \tag{28}$$

$$p^{\min}_m \le p_{m,t} \le p^{\max}_m \tag{29}$$

D. Constraints of District Heating System

Steam and hot water are commonly used as heat transfer media in district heating system. The heat network is regarded as a fluid network where node flow balance, node power fusion, load take-up characteristics, supply and return water temperature constraints, and pipe section heat transfer characteristics are considered. The details of the model can be found in [31], [32].

$$\sum_{n\in S^{pipe+}_m} Q^{g}_{n,t} = \sum_{o\in S^{pipe-}_m} Q^{g}_{o,t} \tag{30}$$

$$\sum_{n\in S^{pipe+}_m} T^{O}_{n,t} Q^{g}_{n,t} = T^{I}_{o,t} \sum_{o\in S^{pipe-}_m} Q^{g}_{o,t} \tag{31}$$

$$h^{L}_{m,t} = cQ^{g}_{m,t}\left(T^{g}_{m,t} - T^{h}_{m,t}\right) \tag{32}$$

$$T^{g}_{\min} \le T^{g}_{m,t} \le T^{g}_{\max} \tag{33}$$

$$T^{h}_{\min} \le T^{h}_{m,t} \le T^{h}_{\max} \tag{34}$$

$$T_e = \left(T_a - T_s\right)x\left(Rc\rho f\right)^{-1} + T_s \tag{35}$$

IV. Simulation Results and Analysis

A. Basic Data

This paper performs simulation and optimization analysis based on MATLAB and GAMS platform in the win10 operation system, i7CPU, 2.20 GHz processor environment. The structure of IES discussed in the example is shown in Fig. 3.

IES is composed of the following three parts: modified IEEE 14-node electric power distribution system, IEEE 11-node natural gas distribution system [33], and modified district heating system based on [17]. The energy flow is interacted through the energy coupling unit, which is located at the coupling node formed by the 4-node electric power distribution system; the 7-node natural gas distribution system; and the 8-node district heating system. The natural gas flow is converted to the power by the heat value. The power generation cost and natural gas price can be found in [34]. The fixed time-interval for real-time dispatching optimization takes 5 min and 1 min, respectively. The parameters of the devices can be found in [35]. Relevant operation constraints are as follows:

1) In electric power distribution system, the nodal voltage is kept between 0.95-1.05 p.u..

2) In natural gas distribution system, the minimum pressure is 22.5 mbar, and the upper limit of pipeline 12-14 flow is 150 m^3/h.

3) In district heating system, the maximum mass flow allowed in the pipeline is 1.6 kg/s, the upper and lower limits of the water supply temperature are 70 ℃ and 69 ℃, and the upper and lower limits of the return water temperature are 30 ℃ and 29 ℃, respectively. In consideration of thermal inertia, a deviation of ± 1 ℃ is allowed for the supply temperature.

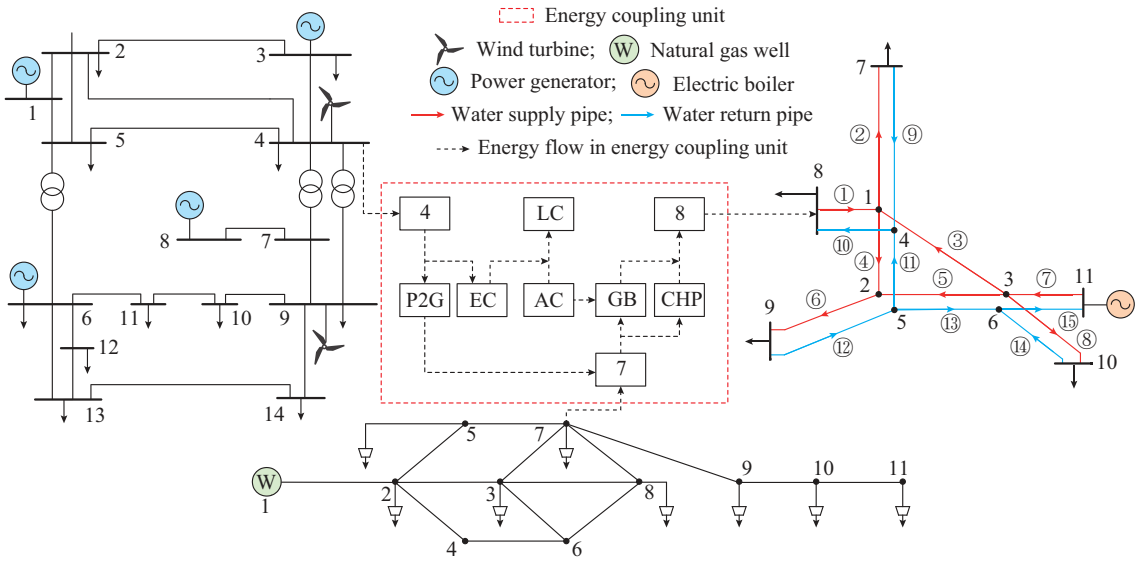

Fig. 3. Example system of IES.

B. Effectiveness Analysis

1) Case 1: Analysis of Configuration Results

S1: IES dispatching based on dynamic time-interval of MPC. In the case, the set of prediction time domain is 1440 min and the control time domain is at least 1 min. Due to the setting of decision index of dynamic time-interval, the control interval is not fixed. According to the dispatching principle of IESs based on dynamic time-interval of MPC given in Section II-A, the real-time dispatching instruction and dispatching sequence at t_{k+1} will be given at time t_k, and the subsequent dispatching plan at t_{k+1} will continue to be calculated. A total of 787620 iterations are eventually spent to complete the one-day dispatching and give the dispatching curve. Based on the electricity, gas, heat, and cold load data of a certain place in Germany [36], the day-ahead dispatching plan and real-time dispatching plan shown in Fig. 4 are obtained through the dispatching process in Section II-D.

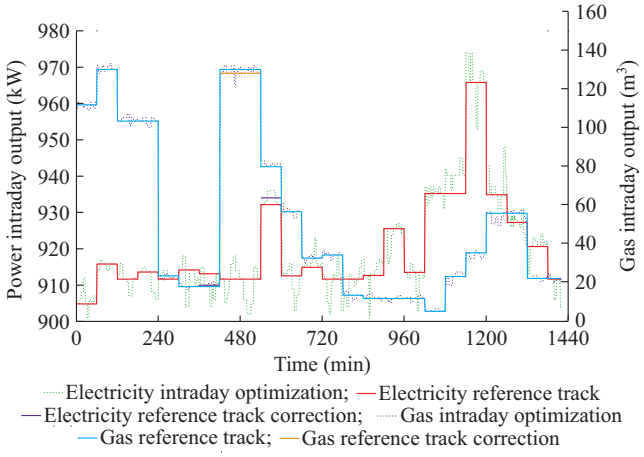

Fig. 4. Dispatching plan of IES.

The dispatching results in the period of 18:00-21:00 are used as a display, and the results are shown in Fig. 5.

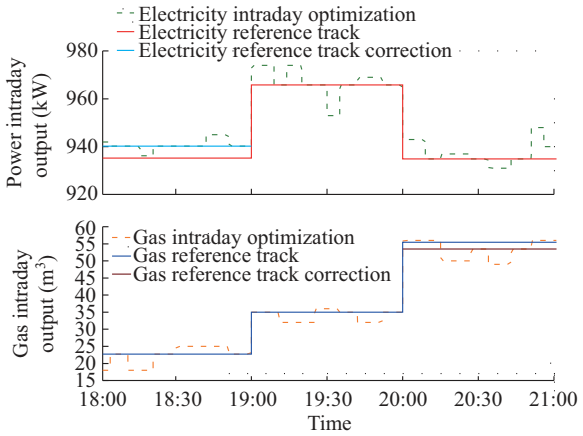

Fig. 5. Dispatching results of IES based on dynamic time-interval of MPC during the period of 18:00-21:00.

The dynamic dispatching with 1 min as the step size is shown in Fig. 5. When the system error is small at 18:03-18:12, 18:21-18:30, 18:51-19:00, 19:53-20:00, 20:43-20:51, etc., the dispatching can be done according to the previous plan without redundant dispatching instruction. When the system error is large at 18:13-18:20, 18:30-18:50, 19:01-19:52, 20:01-20:42, 20:52-21:00, etc., we make dispatching corrections. The reference trajectory of electric output between 18:00-19:00 and the reference trajectory of natural gas output between 20:00-20:45 are corrected. The real-time loads of these two time periods are quite different from the loads predicted before. If the original day-ahead plan is used as a reference trajectory, the performance index will be greatly affected after the optimization. Therefore, the reference trajectory is corrected to make the reference value more accurate.

2) Case 2: Effectiveness Analysis of Decision Index of Dynamic Time-interval

The results of MPC dispatching at fixed intervals of 5 min/1 min are compared with the IES dispatching based on dynamic time-interval of MPC in Case 1.

S2: IES dispatching based on fixed time-interval of 5 min

S3: IES dispatching based on fixed time-interval of 1 min

In the model of Section II-C, the decision index of dynamic time-interval is not considered, and 5 min and 1 min are used as the time-interval of dispatching , respectively. Other conditions and solutions are the same as those in S1, and the dispatching results are solved. The results of S2 and S3 during 18:00-21:00 are shown in Figs. 6 and 7.

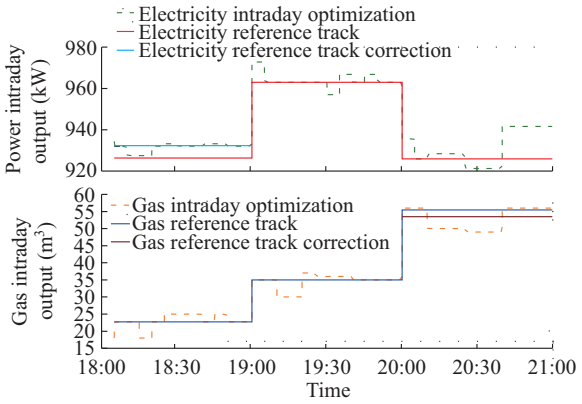

Fig. 6. Dispatch results at a fixed interval of 5 min during 18:00-21:00.

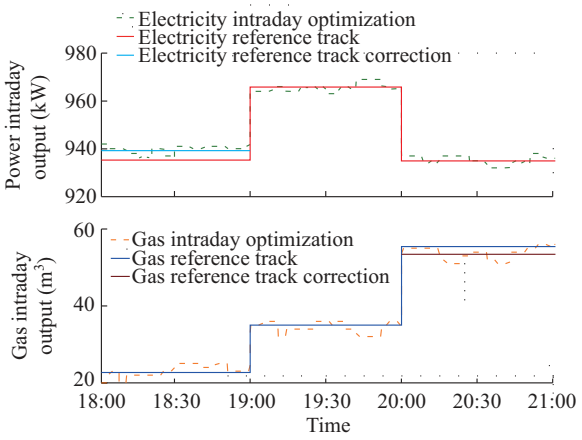

Fig. 7. Dispatching results at a fixed interval of 1 min during 18:00-21:00.

The dispatching results based on MPC with the fixed time-interval of 5 min and 1 min are compared and analyzed. Table I shows the results of performance indexes of the dispatching in one day in S1, S2, and S3.

TABLE I
COMPARISON OF PERFORMANCE INDEXES FOR S1, S2 AND S3

Scene	Real-time deviation (kW)	Reconciling incremental cost ($)	Dispatching cost ($)
S1	116.42	2154.24	30145.73
S2	151.89	591.36	32259.68
S3	72.25	3822.72	32285.35

According to Figs. 5-7 and Table I, compared with S1 and S2, the real-time deviation and real-time dispatching cost of S1 effectively reduce, but the incremental adjustment cost increases. This is because the 1-min time step in S1 is more meticulous than the 5-min time step for S2. S1 can track the load deviation of 1 min in real time and sense the load change within 5 min. This enables S1 to realize real-time adjustment of the unit and min-level adjustment of load demand to reduce unnecessary demand response costs. Therefore, the dispatching cost and real-time deviation of S1 have been reduced. However, since the time step size of S1 is smaller than S2, the number of adjustments increases, which increases the adjustment incremental cost of S1. Overall, compared with S2, the real-time deviation and dispatching cost in S1 are reduced by 23.35% and 6.55%, respectively. The incremental adjustment cost increases by 264.29%.

Compared with S3, the adjustment incremental cost and real-time dispatching cost of S1 are effectively reduced, but the real-time deviation is not as good as that in S3. The main reason is that the real-time 1-min fixed time-interval dispatching is meticulous, and each 1-min time step is adjusted, which makes the system respond to the 1-min load demand. And the real-time deviation is reduced. Although the time step size of S1 is also 1 min, due to the role of decision index of dynamic time-interval, no dispatching instruction is applied at some unnecessary time steps, which makes the dispatching time of S3 increase compared to that of S1. Therefore, the real-time deviation of S3 is small, and the incremental adjustment cost and real-time dispatching cost are high. Overall, compared to S3, the real-time deviation of S1 increases by 61.13% and the incremental adjustment cost and dispatching cost decrease by 43.65% and 6.63%, respectively.

3) Case 3: Effectiveness Analysis of Correction Index of Reference Trajectory

S4 represents IES dispatching based on dynamic time-interval of MPC without considering the correction index of reference trajectory. In the model of Section II-C, the correction index of reference trajectory is not considered, and other conditions and solutions are the same as those in S1. The dispatching results are solved. Figure 8 shows the dispatching results during 18:00-21:00. Table II shows the dispatching results of performance indexes in S1 and S4.

According to Fig. 8 and Table II, S1 is smaller than S4 in real-time deviation, adjustment incremental cost, and real-time dispatching cost. This is because S4 does not consider the correction index of reference trajectory, and the system is always based on the original day-ahead plan. The performance index is the target for optimal dispatching. However, due to the large changes in the electrical load during 04:00-05:00, 07:00-08:00 and 06:00-08:00, 19:00-20:00, the significance of the optimal plan of the original day-ahead plan is reduced. The non-optimal reference trajectory of the original day-ahead plan, results in excessive optimization of performance index for real-time deviation, adjustment of incremental costs, and real-time dispatching costs. Therefore, it is difficult to ensure that the system is globally optimal in the predicted time domain.

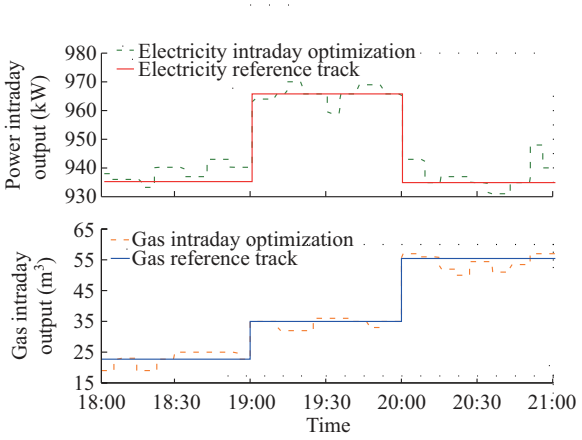

Fig. 8. IES dispatching based on dynamic time-interval of MPC without considering correction index of reference trajectory.

TABLE II
COMPARISON OF PERFORMANCE INDEXES IN S1 AND S4

Scene	Real-time deviation (kW)	Reconciling incremental cost ($)	Dispatching cost ($)
S1	116.42	2154.24	30145.73
S4	125.79	2840.64	31320.05

C. Sensitivity Analysis

1) Case 4: Influence of Decision Indexes of Different Dynamic Time-intervals on Dispatching Results

S5 represents IES dispatching based on different decision indexes of dynamic time-interval of MPC. In the model of Section II-C, five groups of ξ_t are set, which are 0.04, 0.08, 0.12, 0.16, and 0.20, respectively. If the current value is less than the set value, the decision of dynamic time-interval is not triggered, vice versa. Other conditions and solutions are the same as those in S1. The dispatching results are solved. The results of the performance index change with the decision index of dynamic time-interval, which is shown in Fig. 9.

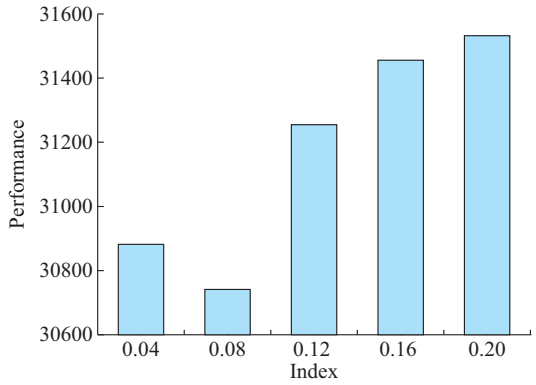

Fig. 9. Dispatching results for different decision indexes of dynamic time-interval.

Different values of the decision index of dynamic time-interval will have different effects on the optimization of the system performance index. When the decision index of dynamic time-interval is too large, the change detection of the system state error is not obvious, which leads to an increase in the trajectory deviation and the performance index. When the decision index of dynamic time-interval is too small, the system state error is easier to be detected, which leads to frequent dispatching. Although it is beneficial to reduce the trajectory deviation, it increases the control energy and control cost, and the performance index increases. Therefore, in Fig. 9, as the decision index of dynamic time-interval increases, the performance index first decreases and then increases.

2) Case 5: Impact of Different Correction Indexes of Reference Trajectory on Dispatching Results

S6 represents IES dispatching based on dynamic time-interval of MPC with different correction indexes of reference trajectory. In the model of Section II-C, five sets of ς_t are set, which are 0.04, 0.08, 0.12, 0.16, and 0.20, respectively. If the correction index value of reference trajectory for the current state is less than this value, the correction decision of reference trajectory is not triggered, vice versa. Other conditions and solutions are the same as those of S1. The dispatching results are solved. The results of performance index change with the reference trajectory correction index, which is shown in Fig. 10.

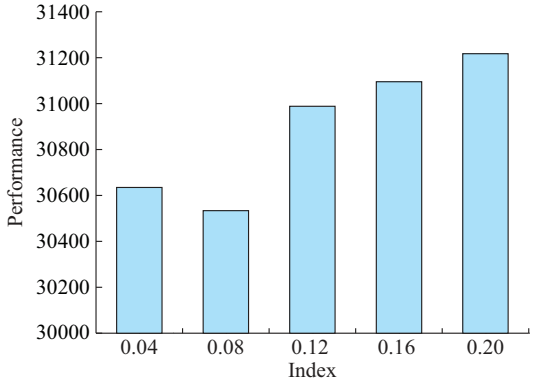

Fig. 10. Dispatching results of different correction indexes of reference trajectory.

The different values of the correction indexes of reference trajectory will affect the correction of the day-ahead plan when optimizing the dispatching in real time. When the correction index of reference trajectory is large, the deviation margin between the actual trajectory and the reference trajectory is large. Therefore, some necessary corrections may be lost, and the trajectory deviation in the performance index increases. When the correction index of reference trajectory is small, the deviation margin between the actual trajectory and the reference trajectory is small. Some unnecessary corrections may be performed, which increase the control energy and control cost in the performance index. According to Fig. 10, as the correction index of reference trajectory increases, the performance index decreases first and then increases. The decrease is due to the enlarged deviation margin and the reduced control energy and control cost. The increase is due to further enlargement of the deviation margin, which greatly increases the trajectory deviation of the system.

3) Case 6: Analysis on Change Level of Natural Gas Storage and Advance Storage Sensitivity

The diversity of operation modes of IESs is largely derived from natural gas storage, due to its time-shifting characteristics. The change level and the ability to store in advance are the key factors that affect the dispatching results of IESs. Therefore, in the analysis of the proposed dispatching sensitivity, we also consider the change level and the sensitivity of natural gas storage in advance.

S7 represents IES dispatching without MPC. Regardless of the MPC method, 1 min is used as the dispatching interval, and the dispatching results are solved based on the same basic data as those of S1. The comparison of natural gas deposits for S1 and S7 is shown in Fig. 11.

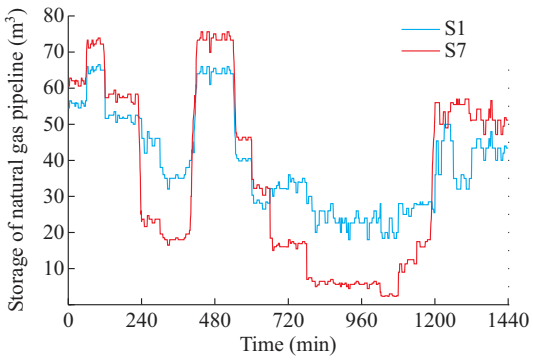

Fig. 11. Storage of natural gas pipeline for S1 and S7.

In Fig. 11, the storage of natural gas pipeline in S1 has been maintained at a relatively high level around 360 min and 1080 min, and reserves for the peak load of about 480 min and 1200 min. After reaching the peak of the load, the pipeline storage slowly decreases. In S2, in the face of the peak load, the pipeline storage rapidly rises at around 420 min and 1140 min. After the peak load, it drops rapidly and maintains at a low level. We quantify the change of pipeline storage and the store sensitivity in advance by γ and μ. We define γ as the ratio of the peak-to-valley difference of the pipeline storage to the time-interval between peaks and valleys. The smaller the value, the smoother the curve of natural gas pipeline storage. μ is defined as the ratio of the difference between the peak and valley moments of the pipeline storage and the difference between the peak and valley values. The larger the value, the better the ability to make advance preparations for load peaks. γ and μ are shown in (36) and (37).

$$\gamma = \frac{\max(L_t) - \min(L_t)}{|t(\max(L_t)) - t(\min(L_t))|} \tag{36}$$

$$\mu = \frac{|t(\max(L_t)) - t(\min(L_t))|}{\max(L_t) - \min(L_t)} \tag{37}$$

The change of pipeline storage and the store sensitivity in advance of S1 and S7 are shown in Table III. Compared with S7, the change of pipeline storage in S1 decreases by 50%, and the store sensitivity in advance increases by 102.27%. S1 has a smoother change in pipeline storage than S7, and the store sensitivity in advance is higher. When the natural gas load reaches the peak value, the natural gas pipeline storage can be maintained at a high level for peak load by the dispatching method proposed in this paper. The changes of pipeline storage are smoothed. It can reserve in advance for the peak load demand in the future; stabilize the pressure of the natural gas pipeline to a certain extent; reduce the failure of gas network equipment; and play a positive role in the safe operation of the system.

TABLE III
COMPARISON OF CHANGE OF PIPELINE STORAGE AND STORE SENSITIVITY IN ADVANCE IN S1 AND S7

Scene	γ	μ
S1	0.06	16.91
S7	0.12	8.36

V. CONCLUSION

In this paper, a dispatching method for IES based on dynamic time-interval of MPC is proposed. Taking trajectory deviation control and energy control costs as the performance index, an decision index of dynamic time-interval is established to ensure timely and accurate dispatching of the system. A correction index of reference trajectory is established to ensure that the system achieves global optimal dispatching with dynamic and hybrid time scales in the prediction time domain. The dispatching process of IES based on dynamic time-interval of MPC is described. Finally, the effectiveness of the proposed dispatching method is validated through case studies. The following conclusions can be drawn based on the study results.

1) The decision index of dynamic time-interval can judge whether the system needs timely control instructions according to the system status. It can help the system dispatching in real time when the system deviation is large and reduce unnecessary dispatching when the system deviation is small. It is helpful to ensure dispatching accuracy and reduce unnecessary dispatching costs. Compared with the fixed time-intervals of 5 min and 1 min, the dispatching cost of IES deceases by 6.55% and 6.63%, respectively.

2) The correction index of reference trajectory can correct the day-ahead plan when the real-time dispatching is significantly different from the day-ahead plan. Compared with the fixed interval of 5 min, the real-time deviation of the dynamic time-interval of MPC for IES dispatching decreases by 23.35%.

3) Decision index of dynamic time-interval and correction index of reference trajectory need to adjust the margin according to the actual needs of the system. As the values of decision index of dynamic time-interval and the correction index of reference trajectory increase, the performance index changes into a concave curve shape. Too high or too low margins will increase the performance index.

4) Compared with the dispatching method without MPC, the dispatching method for IESs based on dynamic time-interval of MPC has advantages in smoothing pipeline changes and storing in advance. The change in the inventory decreases by 50%, and the store sensitivity in advance increases by

102.27%, which is conducive to protect the safety of natural gas pipelines.

REFERENCES

[1] C. Shao, Y. Ding, J. Wang *et al*., "Modeling and integration of flexible demand in heat and electricity integrated energy system," *IEEE Transactions on Sustainable Energy*, vol. 9, no. 1, pp. 361-370, Jan. 2017.

[2] W. Wang, D. Wang, H. Jia *et al*., "Review of steady-state analysis of typical regional integrated energy system under the background of energy internet," *Proceedings of the CSEE*, vol. 36, no. 12, pp. 3292-3305, Jun. 2016.

[3] J. Mei, Z. Wei, Y. Zhang *et al*., "Dynamic optimal dispatch with multiple time scale in integrated power and gas energy systems," *Automation of Electric Power Systems*, vol. 42, no. 13, pp. 36-42, Jul. 2018.

[4] Y. Zhang, Y. Rui, K. Zhang *et al*., "Consumption behavior analytics-aided energy forecasting and dispatch," *IEEE Intelligent Systems*, vol. 32, no. 4, pp. 59-63, Aug. 2017.

[5] C. Wang, B. Hong, L. Guo *et al*., "A general modeling method for optimal dispatch of combined cooling, heating and power microgrid," *Proceedings of the CSEE*, vol. 33, no. 31, pp. 26-33, Nov. 2013.

[6] Z. Wei, S. Zhang, G. Sun *et al*., "Carbon trading based low-carbon economic operation for integrated electricity and natural gas energy system," *Automation of Electric Power Systems*, vol. 40, no. 15, pp. 9-16, Aug. 2016.

[7] Y. Jiang, X. Jian, Y. Sun *et al*., "Day-ahead stochastic economic dispatch of wind integrated power system considering demand response of residential hybrid energy system," *Applied Energy*, vol. 190, pp. 1126-1137, Jan. 2017.

[8] J. Guanetti, S. Formentin, and S. M. Savaresi, "Energy management system for an electric vehicle with a rental range extender: a least costly approach," *IEEE Transactions on Intelligent Transportation Systems*, vol. 17, no. 11, pp. 3022-3034, Nov. 2016.

[9] X. Jin, Y. Mu, H. Jia *et al*., "Optimal day-ahead dispatch of integrated urban energy systems," *Applied Energy*, vol. 180, pp. 1-13, Feb. 2016.

[10] H. Li, W. Wang, J. Yan *et al*., "Economic assessment of the mobilized thermal energy storage (M-TES) system for distributed heat supply," *Applied Energy*, vol. 104, no. 2, pp. 178-186, Apr. 2013.

[11] X. Dou, W. Zhao, Y. Lang *et al*., "A review of operation of natural gas-electricity coupling system considering power-to-gas technology," *Power System Technology*, vol. 43, no. 1, pp. 165-173, Jan. 2019.

[12] D. Zhu and G. Hug, "Decomposed stochastic model predictive control for optimal dispatch of storage and generation," *IEEE Transactions on Smart Grid*, vol. 5, no. 4, pp. 2044-2053, Jul. 2014.

[13] Z. Bing, H. Tazvinga, and X. Xia. "Switched model predictive control for energy dispatch of a photovoltaic-diesel-battery hybrid power system," *IEEE Transactions on Control Systems Technology*, vol. 23, no. 3, pp. 1229-1236, May 2015.

[14] Z. Bao, Q. Zhou, Z. Yang *et al*., "A multi time-scale and multi energy-type coordinated microgrid scheduling solution – part I: model and methodology," *IEEE Transactions on Power Systems*, vol. 30, no. 5, pp. 2257-2266, Sept. 2015.

[15] Y. Li, H. Zhang, X. Liang *et al*., "Event-triggered-based distributed cooperative energy management for multienergy systems," *IEEE Transactions on Industrial Informatics*, vol. 15, no. 4, pp. 2008-2022, Apr. 2019.

[16] H. Zhang, Y. Li, D. W. Gao *et al*., "Distributed optimal energy management for energy internet," *IEEE Transactions on Industrial Informatics*, vo. 13, no. 6, pp. 3081-3097, Dec. 2017.

[17] S. Yao, W. Gu, X. Zhang *et al*., "Effect of heating network characteristics on ultra-short-term dispatch of integrated energy system," *Automation of Electric Power Systems*, vol. 42, no. 14, pp. 89-96, Jul. 2018.

[18] G. Valverde and T. V. Cutsem, "Model predictive control of voltages in active distribution networks," *IEEE Transactions on Smart Grid*, vol. 4, no. 4, pp. 2152-2161, Dec. 2013.

[19] E. F. Camacho and C. Bordons, *Model Predictive Control*, 1st ed. Berlin: Springer, 2004, pp. 1-11.

[20] J. Wu, B. Zhang, W. Ke *et al*., "Optimal economic dispatch model based on risk management for wind-integrated power system," *IET Generation Transmission & Distribution*, vol. 9, no. 15, pp. 2152-2158, Nov. 2015.

[21] F. Sossan, E. Namor, R. Cherkaoui *et al*., "Achieving the dispatchability of distribution feeders through prosumers data driven forecasting and model predictive control of electrochemical storage," *IEEE Transactions on Sustainable Energy*, vol. 7, no. 4, pp. 1762-1777, Oct. 2017.

[22] B. V. Solanki, A. Raghurajan, K. Bhattacharya *et al*., "Including smart loads for optimal demand response in integrated energy management systems for isolated microgrids," *IEEE Transactions on Smart Grid*, vol. 8, no. 4, pp. 1739-1748, Jul. 2017.

[23] S. Gros, D. Jakus, J. Vasilj *et al*., "Day-ahead scheduling and real-time economic MPC of CHP unit in microgrid with smart buildings," *IEEE Transactions on Smart Grid*, vol. 10, no. 2, pp. 1992-2001, Mar. 2019.

[24] W. Fei, L. Zhou, R. Hui *et al*., "Multi-objective optimization model of source-load-storage synergetic dispatch for a building energy management system based on TOU price demand response," *IEEE Transactions on Industry Applications*, vol. 54, no. 2, pp. 1017-1028, Apr. 2018.

[25] M. Ma, C. Zhang, X. Liu *et al*., "Distributed model predictive load frequency control of multi-area power system after deregulation," *IEEE Transactions on Industrial Electronics*, vol. 64, no. 6, pp. 5129-5139, Jun. 2017.

[26] M. A. Abdullah, K. M. Muttaqi, D. Sutanto *et al*., "An effective power dispatch control strategy to improve generation schedulability and supply reliability of a wind farm using a battery energy storage system," *IEEE Transactions on Sustainable Energy*, vol. 6, no. 3, pp. 1093-1102, Jul. 2015.

[27] B. Chen, Z. Ye, C. Chen *et al*., "Toward a synthetic model for distribution system restoration and crew dispatch," *IEEE Transactions on Power Systems*, vol. 34, no. 3, pp. 2228-2239, May 2019.

[28] C. Shao, D. Yi, J. Wang *et al*., "Modeling and integration of flexible demand in heat and electricity integrated energy system," *IEEE Transactions on Sustainable Energy*, vol. 9, no. 1, pp. 361-370, Jan. 2017.

[29] Z. Wei, S. Zhang, G. Sun *et al*., "Power-to-gas considered peak load shifting research for integrated electricity and natural-gas energy systems," *Proceedings of the CSEE*, vol. 37, no. 16, pp. 4601-4609, Aug. 2017.

[30] C. M. Correa-Posada and P. Sánchez-Martín, "Integrated power and natural gas model for energy adequacy in short-term operation," *IEEE Transactions on Power Systems*, vol. 30, no. 6, pp. 3347-3355, Nov. 2015.

[31] Z. Li, W. Wu, M. Shahidehpour *et al*., "Combined heat and power dispatch considering pipeline energy storage of district heating network," *IEEE Transactions on Sustainable Energy*, vol. 7, no. 1, pp. 12-22, Jan. 2016.

[32] Z. Li, W. Wu, J. Wang *et al*., "Transmission-constrained unit commitment considering combined electricity and district heating networks," *IEEE Transactions on Sustainable Energy*, vol. 7, no. 2, pp. 480-492, Apr. 2016.

[33] M. Abeysekera, J. Wu, N. Jenkins *et al*., "Steady state analysis of gas networks with distributed injection of alternative gas," *Applied Energy*, vol. 164, pp. 991-1002, Feb. 2016.

[34] S. Pazouki and M. R. Haghifam, "Optimal planning and dispatch of energy hub in presence of wind, storage and demand response under uncertainty," *International Journal of Electrical Power & Energy Systems*, vol. 80, pp. 219-239, Jan. 2016.

[35] W. Wang, D. Wang, H. Jia *et al*., "Steady state analysis of electricity-gas regional integrated energy system with consideration of NGS network status," *Proceedings of the CSEE*, vol. 37, no. 5, pp. 1293-1304, Mar. 2017.

[36] DIW Berlin. (2019, May). DIETER. [Online]. Available: https://www.diw. de/de/diw_01. c. 508843. de/forschung_beratung/nachhaltigkeit/umwelt/verkehr/energie/modelle/dieter/dieter. html

Xun Dou received the B.S., M.S. and Ph.D. degrees from Southeast University, Nanjing, China, in 2001, 2004 and 2012, respectively. She has been an Associate Professor at Nanjing Tech University, Nanjing, China. From 2015 to 2016, she was a Visiting Scholar at the School of Mechanical Engineering, University of California, Los Angeles (UCLA), Los Angeles, USA. She is the author of more than 20 articles, and more than 10 inventions. Her research interests include integrated energy systems, power markets and power economics, demand response, and power planning.

Jun Wang received the B.S. degree in electrical engineering and automation from Nanjing Tech University, Nanjing, China, in 2017. He is currently pursuing the M.S. degree in the College of Electrical Engineering and Control Science, Nanjing Tech University. His research interests include integrated energy systems, and power markets and power economics.

Zhen Wang is now working toward the B.S. degree in electrical engineer-

ing and automation at the Nanjing Tech University, Nanjing, China. His research interests include integrated energy systems, and microgrid optimal operation.

Lijuan Li received the B.S. and M.S. degrees from Nanjing Tech University, Nanjing, China, in 1997 and 2004, respectively, and Ph.D. degree at the Zhejiang University, Hangzhou, China, in 2008. She has been a Professor at Nanjing Tech University. From 2013 to 2014, she was a Visiting Scholar at the University of California, USA. Her research interests include data science, the application of artificial intelligence in industrial processes, modeling of complex industrial processes, predictive control, and control system performance evaluation.

Linquan Bai received the B.S. and M.S. degrees in electrical engineering from Tianjin University, Tianjin, China, in 2010 and 2013, respectively, and Ph.D. degree at the University of Tennessee, Knoxville, USA. He is an Assistant Professor at University of North Carolina at Charlotte, Charlotte, USA. His research interests include power system operation and optimization, electricity markets, and integrated energy systems.

Shuhui Ren received the B.S. degree in electrical engineering and automation from Nanjing Tech University, Nanjing, China, in 2019. She is currently pursuing the M.S. degree in the College of Electrical Engineering and Control Science, Nanjing Tech University. Her research interests include integrated energy systems, and integrated demand response.

Min Gao received the Ph.D. degree in electrical engineering and the M.S. degree in electrical engineering from University of California, Los Angeles, USA, and the B.E. degree in electrical engineering and automation, Nanjing Tech University, Nanjing, China. He was a Visiting Scholar with Max Planck Institute for Software Systems, Germany, and State Key Laboratory of VLSI and Systems, Fudan University, Shanghai, China. His research interests include Energy Internet, machine learning, formal verification, cloud computing, internet of things, and hetrogeneous computing.